Spin polarization in quantum wires: Influence of Dresselhaus spin-orbit interaction and cross-section effects

L. Villegas-Lelovsky,[1,2] C. Trallero-Giner,[3] M. Rebello Sousa Dias,[2] V. Lopez-Richard,[2] and G. E. Marques[2]
[1]*Departamento de Ciências Físicas, Universidade Federal de Uberlândia, 38400-902 Uberlândia, Minas Gerais, Brazil*
[2]*Departamento de Física, Universidade Federal de São Carlos, 13560-905 São Carlos, São Paulo, Brazil*
[3]*Departamento de Física Teórica, Universidad de La Habana, 10400 Havana, Cuba*
(Received 6 November 2008; revised manuscript received 14 February 2009; published 8 April 2009)

We examine the effects of the *full* Dresselhaus spin-orbit coupling on laterally confined quantum wire states. An analysis of the relative contributions due to linear, quadratic, and cubic Dresselhaus spin-orbit terms on the energy levels, spin splitting, and spin polarization has been carried out. The effects of wire cross-sectional geometry shapes on the electronic structure are explored. In particular we compared the results of semicylindrical and cylindrical confinements and have found important differences between the spin degeneracy of the ground-state level and the spin-polarization dependence on sign inversion of the free linear momentum quantum number along the wire axis. Different from other symmetries, in both cases here considered, the stronger spin-splitting effects come from the quadratic Dresselhaus term. We report ideal conditions for realization of spin-field filter devices based on symmetry properties of the spin splitting of the ground state in semicylindrical quantum wires.

DOI: 10.1103/PhysRevB.79.155306 PACS number(s): 73.21.Hb, 71.70.Ej, 73.22.Dj, 72.25.Dc

I. INTRODUCTION

Bulk spin-orbit interaction (SOI) effects of zinc-blende crystals have been discussed in earlier theoretical papers.[1–3] They break the spin degeneracy of the Bloch states for every wave vector **k** in the absence of a center of inversion and lead to the energy spin splitting of the electron and/or hole states without lifting Kramer's degeneracy in the absence of an external magnetic field. In low dimensional heterostructures, this spin splitting can be tuned by external field and classified into two effects either induced by bulk inversion asymmetry (BIA) in zinc-blende crystal structures, known as Dresselhaus SOI, and/or by structure inversion asymmetry (SIA) of the confinement potential.

The intrinsic form of BIA SOI which affects the energy level separation of carrier states in zinc-blende nanostructures can be detected via spin-polarized optical and transport measurements. Recently, the BIA-induced spin splitting has been detected experimentally through the Shubnikov–de Haas effect in uniaxially strained bulk InSb and by analyzing the precession of the spin polarization of photoexcited electrons along the (110) GaAs surfaces.[4] In turn, SIA-induced spin splitting has been detected via analysis of optical polarized emissions from electron and hole charge densities accumulated in layers of GaAs-AlAs tunneling diodes[5] under applied parallel electric and magnetic fields.

In this work we present a detailed $\mathbf{k}\cdot\mathbf{p}$ analysis of the electronic structure in semiconductor quantum wires (QWRs) of different geometrical shapes after including all Dresselhaus SOI terms in the Hamiltonian for the conduction band states which contain the *full* symmetry of the crystal.[3,6,7] QWRs have attracted attention because of their potential applications in spintronic and optoelectronic devices. The study of these systems allows us to understand the role played by dimensionality,[8] by electron-electron interaction,[9] as well as by size and shape quantization effects on their electronic properties.[10,11]

In general, the Dresselhaus SOI coupling has been introduced to the electronic structure of nanostructures by taking the mean values of the wave-vector operators $\hat{k}_z^2$ and $\hat{k}_z$, as usually done in quantum dots[12] (QD's) or in a two-dimensional (2D) electron gas in quantum wells (QW's).[4] In most cases, $\langle\hat{k}_z\rangle=0$ and such approaches consider only effects due to in-plane $\hat{k}$-linear terms proportional to the in-plane **k** components (k_x,k_y).[3,8,13,14] For other types of confinements, as well as for materials with a large values of SOI parameters, the $\hat{k}$-cubic term must be included in the total Hamiltonian. Recently, the effect of the k-cubic term has appeared to be relevant even for GaAs-AlGaAs, a system with very small SOI parameters.[15,16] Moreover and due to the translational invariance symmetry of one-dimensional (1D) quantum systems along the z axis, the BIA quadratic term, proportional to $\hat{k}_z$, should also have a relevant contribution to the electronic subband structure of QWRs.

Later on we shall discuss why SOI quadratic and cubic terms are essential to determine eigenenergies, spin-splitting energies, and spin polarizations of electrons in the conduction band of QWRs. By changing the ratio between SOI and quantum confinement strengths we can follow the relative influences of each BIA term on the electronic spectra. Furthermore, besides the qualitative differences between circular and semicircular cross-section QWRs, we will also show that any symmetry reduction leads to a set of eigenstates affected by different combinations of SOI linear, quadratic, and cubic Dresselhaus contributions. Hence, symmetry considerations to determine the Hilbert space for the solutions used in the expansion of the spinor states and the relative effects between different SOI terms become the main issue under discussion in this work. In this study, we will focus on the interplay between linear, quadratic, and cubic BIA contributions to the spin-splitting energy and the corresponding spin polarization of the ground state of nanoscopic QWRs. In our analysis we have found that the $\hat{k}$-linear and $\hat{k}$-cubic terms keep the degeneracy of the eigenenergies in a semicylindrical QWR and, in consequence, their contribution to the spin-splitting energy is negligible. Finally, we addressed the ef-

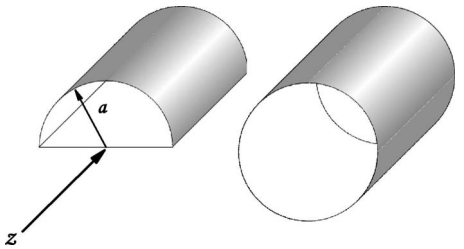

FIG. 1. Quantum wire systems with semicylindrical and cylindrical geometric cross sections.

fects associated to the reduction in the cylindrical symmetry on the dependence of the ground-state energy on the sign of wave vector k_z along the propagation direction and its notably high degree of spin polarization at low velocity values.

II. INFINITE QUANTUM WIRE SYSTEMS

The total single-particle Hamiltonian for the conduction band of a QWR, including *all* Dresselhaus SOI contributions, can be written as

$$\mathcal{H} = \mathcal{H}_0 + \mathcal{H}_D, \tag{1}$$

where $\mathcal{H}_0=[\hbar^2\hat{\mathbf{k}}^2/2m^*+V(\mathbf{r},z)]I$ is the Hamiltonian for uncoupled *spin-up* and *spin-down* electron states, I is the 2×2 identity matrix, $V(\mathbf{r},z)$ is the total spatial confinement for Cartesian coordinates $\mathbf{r}=(x,y)$ and z along the wire axis (see Fig. 1), $\mathcal{H}_D=\beta(\sigma\cdot\hat{\kappa})$ is the BIA Hamiltonian, m^* and β are the electron effective mass and Dresselhaus SOI parameter for the material, respectively, $\sigma=(\sigma_x,\sigma_y,\sigma_z)$ is the Pauli spin-vector matrix, and $\hat{\kappa}$ is a vector operator with $\hat{\kappa}_x=(\hat{k}_y\hat{k}_x\hat{k}_y-\hat{k}_z\hat{k}_x\hat{k}_z)$ and cyclic permutations for the other $\hat{\kappa}_y$ and $\hat{\kappa}_z$ components and of the associated linear momentum operator $\hat{\mathbf{k}}=(\hat{k}_x,\hat{k}_y,\hat{k}_z)$. The effective full BIA Hamiltonian can be separated into three contributions with the form

$$\mathcal{H}_D = \mathcal{E}_0 a^3 \begin{pmatrix} \mathcal{H}_{2D} & \mathcal{H}_{1D}+\mathcal{H}_{3D} \\ \mathcal{H}_{1D}^\dagger+\mathcal{H}_{3D}^\dagger & -\mathcal{H}_{2D} \end{pmatrix}, \tag{2}$$

where $\mathcal{H}_{1D}=-\gamma_D\hat{k}_z^2\hat{k}_-$, $\mathcal{H}_{2D}=-\frac{1}{2}\gamma_D\hat{k}_z(\hat{k}_-^2+\hat{k}_+^2)$, $\mathcal{H}_{3D}=-\frac{1}{8}\gamma_D\{\hat{k}_+,(\hat{k}_+^2-\hat{k}_-^2)\}$, and $\{\hat{A},\hat{B}\}=\frac{1}{2}(\hat{A}\hat{B}+\hat{B}\hat{A})$. These terms are, respectively, the linear, the quadratic, and the cubic Dresselhaus SOI contributions written in terms of operators $\hat{k}_\pm=\hat{k}_x\pm i\hat{k}_y$ multiplied by the dimensionless parameter $\gamma_D=\beta/(a^3\mathcal{E}_0)$, where $\mathcal{E}_0=\hbar^2/(2m^*a^2)$ is the energy scale for the QWR confinement inside a cylinder (or semicylinder) of radius a (see Fig. 1). For free motion along the z axis $[V(\mathbf{r},z)\equiv V(\mathbf{r})]$, we can show that the commutator $[\hat{k}_z,\mathcal{H}]=0$ thus, the eigenvalue of $\hat{k}_z$ operator (k_z) becomes a good quantum number. Under these conditions, the Schrödinger equation for $\mathcal{H}$ is separable, in the entire level spectrum, as a product of purely *in-plane* localized function on the radial coordinate $\mathbf{r}$ times free motion function along z axis. For mathematical simplicity we will assume a hard-wall confining potential model with $V(\mathbf{r})\equiv 0$ inside the region $|\mathbf{r}|<a$ and infinite barrier outside the wire with $V(|\mathbf{r}|\geq a)=\infty$. Without SOI, the eigenenergies of the Hamiltonian in Eq. (1) become degenerate and correspond to the spinor eigenfunctions, $|\psi^+\rangle\equiv\binom{|f_0\rangle|+\rangle}{0}$ and $|\psi^-\rangle\equiv\binom{0}{|f_0\rangle|-\rangle}$, where $|-\rangle$ and $|+\rangle$ are the electron spin-up and spin-down eigenstates of the z component of the spin operator, $\hat{S}_z$. The ket $|f_0\rangle$ can be factorized as $\langle\mathbf{r},z|f_0\rangle=f_0(\mathbf{r},z)=\mathbf{f}(\mathbf{r})\exp(ik_zz)$, where $\mathbf{f}(\mathbf{r})$ is the solution of in-plane Hamiltonian equation,

$$\left[\frac{\hbar^2\nabla_\perp^2}{2m^*}+\frac{\hbar^2k_z^2}{2m^*}\right]f=E_0f, \tag{3}$$

where $\nabla_\perp^2$ is the Laplace operator expressed in polar coordinates, $\mathbf{r}=(\rho,\varphi)$, and E_0 is the eigenvalue of the Hamiltonian $\mathcal{H}_0$ in Eq. (1). The corresponding boundary conditions for a cylinder with circular cross section (right panel of Fig. 1) are given by

$$f(a,\varphi)=0, \quad f(\rho,\varphi)=f(\rho,\varphi+2\pi), \tag{4}$$

and for semicircular cross section (left panel of Fig. 1) by

$$f(a,\varphi)=0, \quad f(\rho,0)=0, \quad f(\rho,\pi)=0. \tag{5}$$

In order to fulfill conditions (4) or (5), the eigensolutions, $f_{n,m}(\rho,\varphi)$, with quantum numbers n and m are products of integer-order Bessel functions, $J_n(u)$, times the corresponding circular eigenfunctions,

$$f_{n,m}=\begin{cases} A_{n,m}^{c}J_n\left(\mu_{n,m}\dfrac{\rho}{a}\right)e^{in\varphi}, & n=0,\pm 1,\pm 2, \\ A_{n,m}^{sc}J_n\left(\mu_{n,m}\dfrac{\rho}{a}\right)\sin(n\varphi), & n=1,2,\ldots . \end{cases} \tag{6}$$

In these expressions, $\mu_{n,m}=\sqrt{(E_0/\mathcal{E}_0-\alpha_z^2)}$ are the mth zero of the nth-order Bessel function, $J_n(\mu_{n,m})=0$, and $\alpha_z=ak_z$. The superscripts, c and sc, label the solutions corresponding to cylindrical and semicylindrical confinements with normalization constants $A_{n,m}^{c}=1/[a\sqrt{\pi}J_{n+1}(\mu_{n,m})]$ and $A_{n,m}^{sc}=2/[a\sqrt{\pi}J_{n+1}(\mu_{n,m})]$, respectively.

The eigenfunctions of the total Hamiltonian $\mathcal{H}$, in Eq. (1), are represented by spinors $|\psi\rangle\equiv\binom{|\psi^+\rangle|+\rangle}{|\psi^-\rangle|-\rangle}$, where the off-diagonal contributions mix spin-up and spin-down components of $\hat{S}_z$. They are determined by the 2×2 Schrödinger equation,

$$\begin{pmatrix} \mathcal{H}_0(k_z)+\mathcal{H}_{2D}(k_z)-\mathcal{E} & \mathcal{H}_{1D}(k_z)+\mathcal{H}_{3D}(k_z) \\ \mathcal{H}_{1D}^\dagger(k_z)+\mathcal{H}_{3D}^\dagger(k_z) & \mathcal{H}_0(k_z)-\mathcal{H}_{2D}(k_z)-\mathcal{E} \end{pmatrix}\begin{pmatrix} |\psi^+\rangle|+\rangle \\ |\psi^-\rangle|-\rangle \end{pmatrix}=0. \tag{7}$$

It is straightforward to show that the functions defined in Eq. (6) form a complete set of orthonormal eigenstates for the spaces determined by Hamiltonian (7) with boundary conditions (4) or (5). Therefore, we can build each component $|\psi^{\pm}\rangle$ of the spinor $|\psi\rangle$ as a linear combination of functions given by Eq. (6),

$$\psi^{\pm}(\rho,\varphi) = \sum_{n,m} C^{\pm}_{n,m} f_{n,m}(\rho,\varphi). \tag{8}$$

In principle, the above expansion yields infinite generalized eigenvalue problems for the Hilbert space of Eq. (7). It becomes clear that each Dresselhaus contribution appearing in $\mathcal{H}$ causes different admixtures between the quantum numbers n and m of the spin-up and spin-down components of spinor states. As will be shown in Secs. III A and III B, the semicylindrical QWR symmetry imposes restrictive conditions on the spin-degenerate energy levels and on the corresponding spin-carrier polarization $\langle \hat{S}_z \rangle$ of the ground state.

III. ENERGY LEVELS AND SPIN CARRIER POLARIZATION

We can search for solutions of $|\psi^{\pm}\rangle$ by direct substitution of expansion (8) into Eq. (7). Then, we end up having to solve an eigenvalue problem, $[\mathbf{H}-I\mathcal{E}]\mathbf{C}=0$, where $\mathbf{H}=(\mathcal{H}_{s,s'})$ is an $(l\times l)$-square matrix (the l value accounts for the convergence of the numerical procedure to solve the secular equation) with elements given by

$$\mathcal{H}_{s,s'} = \begin{pmatrix} (\mu_s^2+\alpha_z^2)\delta_{s,s'} - \frac{1}{2}\gamma_D\alpha_z h_{s,s'} & -\gamma_D\left(\frac{1}{8}j^{+}_{s,s'} + \alpha_z^2 g^{-}_{s,s'}\right) \\ -\gamma_D\left(\frac{1}{8}j^{-}_{s,s'} + \alpha_z^2 g^{+}_{s,s'}\right) & (\mu_s^2+\alpha_z^2)\delta_{s,s'} + \frac{1}{2}\gamma_D\alpha_z h_{s,s'} \end{pmatrix} \tag{9}$$

and $\mathbf{C}=\binom{C^{+}}{C^{-}}$ is a vector that forms the set of eigenstates of the matrix in Eq. (9). The index s represents the set of quantum numbers (n,m), ordered in increasing values of $\mu_{n,m}$. The innermost matrix elements $g^{\pm}_{s,s'}=a\langle s|\hat{k}_{\pm}|s'\rangle$, $h_{s,s'}=a^2\langle s|\hat{k}_{+}^2+\hat{k}_{-}^2|s'\rangle$, and $j^{\pm}_{s,s'}=a^3\langle s|\{\hat{k}^2_{\pm},(\hat{k}^2_{+}-\hat{k}^2_{-})\}|s'\rangle$ can be calculated as shown in the Appendix.

In order to simplify the identification of each state admixture induced by the SOI, let us label the components of a spinor eigenstate as $|n,m;\sigma\rangle$ according to the character of the state at zero BIA interaction given by *pure* or uncoupled $|\sigma=+\rangle$ or $|\sigma=-\rangle$ spin states with eigenvalues $\pm\hbar/2$ along the quantization z axis, respectively. In the sequence, we will be discussing the mixing effects that affect energy levels, spin-splitting energy, and spin polarization caused by the linear, quadratic, cubic, and full Dresselhaus SOI terms for wires with cross sections shown in Fig. 1. It is observed, in Eq. (9), that under the inversion transformation, $k_z \Leftrightarrow -k_z$, we obtain the same conduction subband *mirror* states by only changing spin direction $\sigma\Leftrightarrow-\sigma$. Hence, in Sec. III A we present the electronic spectrum for $k_z \geq 0$ only.

A. Cylindrical cross-section confinement

In the absence of SOI the eigenstates of Eq. (3) for cylindrical QWRs and with boundary conditions given in Eq. (4) have eigenenergies $\mathcal{E}_{n,m}=E_0-\mathcal{E}_0\alpha_z^2=\mathcal{E}_0\mu^2_{n,m}$. These states labeled $|\pm|n|,m;\pm\rangle$ are twofold degenerate for the z component of the angular momentum $n=0$ and fourfold degenerate for $n\neq 0$. The mixing induced by BIA terms in $\mathcal{H}_{\mathcal{D}}$ breaks the spin degeneracy of QWR states in different manners. Following the calculation given in the Appendix we observe that the matrix elements of the off-diagonal linear, $g^{\pm}_{s,s'}$, and cubic, $j^{\pm}_{s,s'}$, Dresselhaus terms [see Eqs. (A2) and (A5)] couple states with opposite spins (interspin coupling) with $\Delta n=n'-n=\mp 1$ and $\Delta n=\mp 3,\pm 1$, respectively. However, the quadratic BIA spin-orbit coupling occurring in the diagonal of Eq. (9), $h_{s,s'}$, connects those states in Eq. (8) with $\Delta n=\pm 2$ [see Eq. (A3)] but inside the same spinor component (intraspin coupling) preserving the spin polarization between coupled quantum numbers (n,m). The energy splitting induced by this quadratic coupling is similar to the Zeeman splitting induced by a magnetic field; besides, it does not mix different n-index parities of the Bessel functions entering the linear combination of Eq. (8).

According to the present selection rules, the Hilbert space for the spinors $\psi^{\pm}(\mathbf{r})$ can be split into two independent subspaces, labeled U and L, which are classified according to the parity of the quantum number n and spin orientation forming the components of each spinor. Thus, the Hilbert subspace U (L) gathers spinor states with spin-up (spin-down) components having *odd* n values (*even* n values) that are coupled with states with spin-down (spin-up) and even n values (odd n values). Hence, the eigenvalue problem for the Hamiltonian in Eq. (7) can be solved independently for each class of states L and U.

In Fig. 2(a) we are showing effects caused by the BIA terms on the first 12 eigenvalues of $\mathcal{H}_0$ as a function of the normalized Dresselhaus parameter $\gamma_D=\beta/(a^3\mathcal{E}_0)$ and for a giving value of the dimensionless wave number $\alpha_z=k_z a$, forming the U class eigenstates. Here, the fourfold degener-

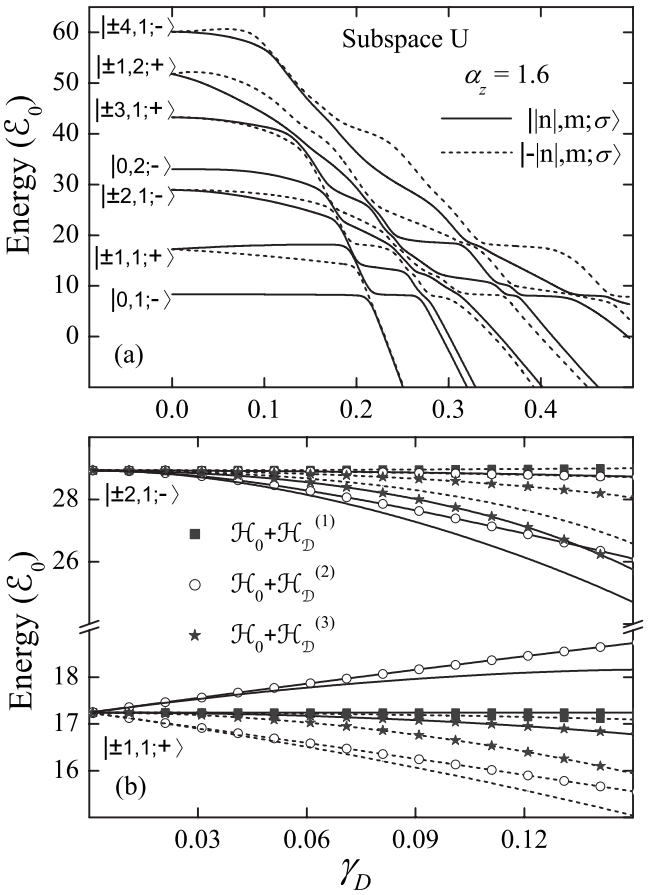

FIG. 2. (a) The first 12 eigenenergies $\mathcal{E}$, in units of $\mathcal{E}_0$ for a cylindrical QWR obtained in the subspace U (labeled as $|n,m;\sigma\rangle$ according to the zero SOI character) as a function of the dimensionless spin-orbit Dresselhaus parameter $\gamma_D=\beta/(a^3\mathcal{E}_0)$ and $\alpha_z=1.6$. Subspace U represents those independent solutions with odd (even) quantum number n and spin up (down). (b) Contribution of the linear (squares), quadratic (circulus), and cubic terms (stars) to the energy of the states $n=\pm1$ and ±2. Here the solid and dashed lines denote, respectively, the full BIA Hamiltonian solutions with quantum number $n\geq0$ and $n<0$, respectively.

ate levels $\mathcal{E}_{\pm n,m}$, in the QWR without SOI, split into twofold degenerate states: $\mathcal{E}_{n,m}^{U,(L)}\Leftrightarrow\mathcal{E}_{-n,m}^{L,(U)}$ for U and L Hilbert subspaces.

After the sequential inclusion of linear, quadratic, and cubic BIA terms, we can assert how substantial is the interplay between these contributions to the electronic structure, as presented in Fig. 2(b). However, by considering only the linear-BIA term without any other contribution, it would not yield any effective energy coupling to this set of levels. For the states $|\pm1,1;+\rangle$, the main contributions are established by the $\mathcal{H}_{2\mathcal{D}}$ and $\mathcal{H}_{3\mathcal{D}}$ *BIA* Hamiltonians. The same results are observed for $|+2,1;-\rangle$, whereas $|-2,1;-\rangle$ suffers stronger changes caused by the cubic SOI term, $\mathcal{H}_{3\mathcal{D}}$. The $\mathcal{H}_{1\mathcal{D}}$ SOI causes practically negligible effect on the eigenenergies, $\mathcal{E}_{|\pm1,1;+\rangle}^{U}$ and $\mathcal{E}_{|\pm2,1;-\rangle}^{U}$.

At this point it is interesting to assert the values of energy spin splitting, for this block of states, induced by the linear, quadratic, cubic, and all-BIA terms taken independently in the Hamiltonian of Eq. (7). Let us label these energy spin-

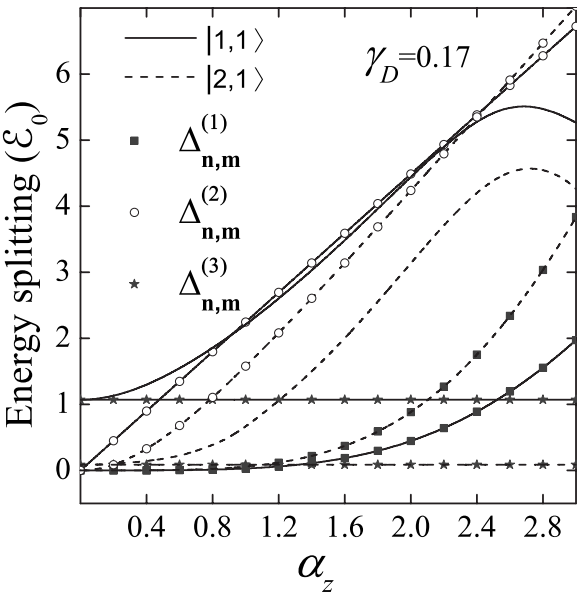

FIG. 3. Energy splitting $\Delta_{1,1}$ (solid line) and $\Delta_{2,1}$ (dashed line) for a cylindrical QWR in units of $\mathcal{E}_0$ as a function of the dimensionless wave vector α_z for $\gamma_D=0.17$. The effects of the SOI linear, quadratic, and cubic BIA terms are indicated by squares, circles, and stars, respectively.

splitting values as $\Delta_{n,m}^{(1)}$, $\Delta_{n,m}^{(2)}$, $\Delta_{n,m}^{(3)}$, and $\Delta_{n,m}$. In Fig. 3 we are presenting the magnitudes of $\Delta_{1,1}^{(i)}$ and $\Delta_{2,1}^{(i)}$ for $i=1,2,3$ and $\gamma_D=1.7$ as a function of the α_z and compared to the total values of $\Delta_{1,1}$ and $\Delta_{2,1}$. This picture characterizes the highly complex interplay between these three contributions. Here, the stronger influence on $\Delta_{1,1}$ and $\Delta_{2,1}$ comes from the quadratic term for $\alpha_z\gtrsim0.6$ and 0.3, respectively. While, for lower values of k_z (α_z smaller than 0.3 and 0.15 for the $|1,1\rangle$ and $|2,1\rangle$ sates) the *predominant* contribution is given by the cubic BIA interaction. Note further that the SOI cubic $\mathcal{H}_{3D}$ term is independent of α_z, whereas the linear component $\mathcal{H}_{1D}$ starts to play a non-negligible contribution to the energy splitting only for large values of k_z ($\alpha_z\propto k_z$).

In order to analyze the induced changes in the spin character of these subbands, we calculate the corresponding spin polarization, defined as $\bar{\sigma}_z^{U,L}(n,m)=\langle\psi_{n,m}^{U,L}|\hat{S}_z|\psi_{n,m}^{U,L}\rangle/|\langle\psi_{n,m}^{U,L}|\psi_{n,m}^{U,L}\rangle|$, for spinors belonging to subspaces U and L. In particular, the spin polarization of ground-state levels, $\bar{\sigma}_z^{L}(0,1)$, is shown in Fig. 4. We have calculate the contour plot of this quantity for $2m\beta/\hbar^2=5$ Å as a function of the QWR radius and momentum k_z. For wires with radius $a>40$ Å there is a large $|k_z|$ interval, centered at $k_z=0$, which shows maximum spin polarization, $\bar{\sigma}_z^{L}(0,1)\cong+1$. This interval becomes narrower as the wire radius increases. Its degenerated mirror state ($k_z\Leftrightarrow-k_z$ and $\sigma_z\Leftrightarrow-\sigma_z$) belonging to the Hilbert subspace U has spin polarization identical to Fig. 4, but with negative $\bar{\sigma}_z^{L}(0,1)$ values. Therefore, there is no net ground-state spin polarization for any given value of k_z once $[\bar{\sigma}_z^{U}(0,1)+\bar{\sigma}_z^{L}(0,1)]\equiv0$ as should be expected for this nonmagnetic material.

B. Semicylindrical cross-section confinement

In order to study the effects associated with spatial shape of the confinement we have used a semicylindrical QWR

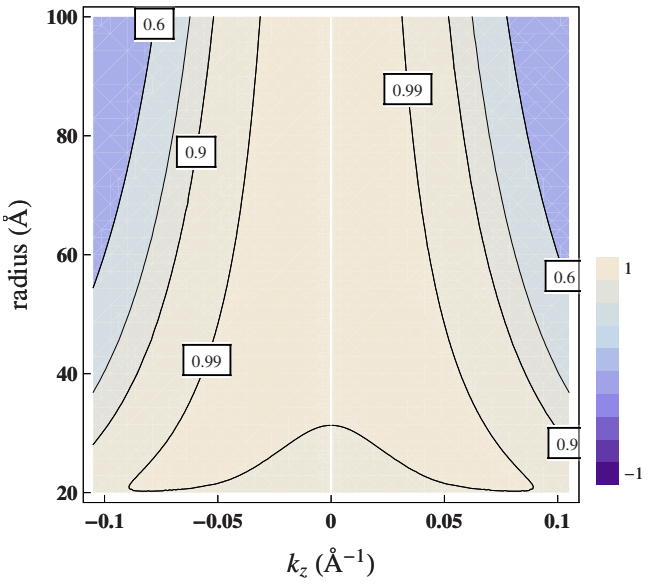

FIG. 4. (Color online) Spin-polarization contours, $\bar{\sigma}_z^L(0,1)$, for the ground state for a cylindrical QWR with Dresselhaus strength $2m\beta/\hbar^2=5$ Å. Here, we changed wavelength k_z and radius a of the QWR.

with reduced symmetry as compared to the cylindrical case. We still may label the states according to the character in the absence of the SOI, namely, $|n,m;\pm\rangle$; however, the solutions now require boundary conditions listed in Eq. (5) and we want to study how many significant modifications are introduced on the electronic spectrum and spin character of the states under this lower symmetry. A first modification is the twofold degeneracy, with eigenenergies $\mathcal{E}_{n,m}=\mathcal{E}_0\mu_{n,m}^2$ at $\gamma_D=0$ (without SOI) for every pair of spin-polarized state $|n,m;\pm\rangle$, with $n>0$. From the Appendix, it is seen that the matrix element for the linear-BIA term, $g_{s,s'}^{\pm}$, couples states with opposite spins but $n'-n=\pm 1$ when n' and n assume odd and even numbers simultaneously [see Eqs. (A7) and (A8)]. The same can be argued for the cubic or interspin, $j_{s,s'}^{\pm}$, and for the quadratic or intraspin, $h_{s,s'}$, BIA coupling elements. In this case the Hilbert space for the spinor $|\psi\rangle$ is not separable and the spin-up and spin-down components are formed by all linear combinations of $n>0$ quantum numbers for each spin orientation.

In Fig. 5(a), we have plotted the first ten energy levels of a semicylindrical QWR, as a function of the dimensionless parameter γ_D, for $\alpha_z=1.6$. The mixing induced by $\mathcal{H}_{\mathcal{D}}$ [see Eq. (2)] breaks the twofold spin degeneracy of the ground state $|1,1;\pm\rangle$, a result different from the obtained for 2D nanostructure states or even in the fully symmetrical cylindrical QWRs as shown in Fig. 2(b). Note that the inclusion of linear ($\mathcal{H}_{1\mathcal{D}}$) and cubic ($\mathcal{H}_{3\mathcal{D}}$) BIA couplings does not break the spin degeneracy of states in semicylindrical wires but only shifts the energy level positions. Moreover, in Fig. 5(a), the crossing between energy levels is lacking, when compared to the cylindrical QWR case, since all the states are coupled by the SOI. All these facts are direct consequences of the spatial asymmetry: the absence of states with $n\leq 0$, the selection of the independent wave functions necessary to describe the semicylindrical QWR spinor state, and the fact that there are only anticrossings (minigaps) between two near energy levels.

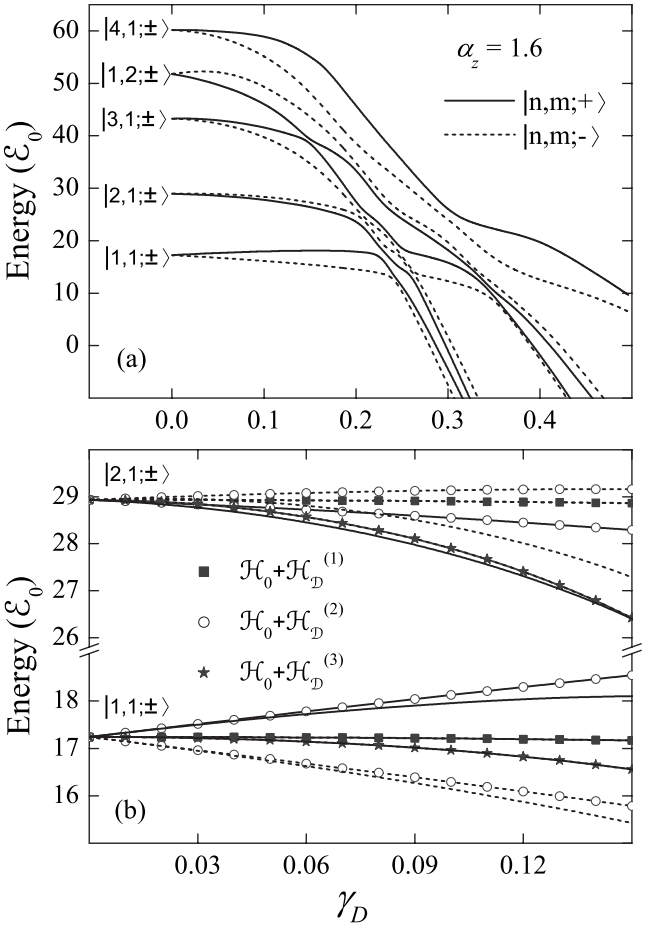

FIG. 5. (a) The first ten eigenenergies $\mathcal{E}$ in units of $\mathcal{E}_0$ for a semicylindrical QWR as a function of the dimensionless spin-orbit Dresselhaus parameter γ_D and $\alpha_z=1.6$. (b) Changes caused by the addition of linear, quadratic, and cubic terms to the energy levels $\mathcal{E}_{1,1;\pm}$ and $\mathcal{E}_{2,1;\pm}$. The same notation of Fig. 2 is used. Solid and dashed lines denote, respectively, the full BIA Hamiltonian solutions with quantum numbers $|n,m;+\rangle$ and $|n,m;-\rangle$.

For a further discussion, we are showing in Fig. 5(b) the influences of the addition of linear, quadratic, and cubic BIA terms on the value of the ground-state and first excited state energies, $\mathcal{E}_{|1,1;\pm\rangle}$ and $\mathcal{E}_{|2,1;\pm\rangle}$. Note that the largest spin splitting of the levels $\mathcal{E}_{|1,1;\pm\rangle}$ is induced by the intraspin term $\mathcal{H}_{2\mathcal{D}}$, whereas the interspin term $\mathcal{H}_{3\mathcal{D}}$ is responsible for the larger curvature of the state $|1,1;+\rangle$. The same observations are valid for the excited states $|2,1;\pm\rangle$ but here, the cubic term is responsible for the strongest modifications. As in the case of the cylindrical QWR, the contribution from the $\mathcal{H}_{1\mathcal{D}}$ term to the energy of all semicylindrical QWR states is negligible, another remarkable contrast to the effects induced by SOI linear-BIA term in 2D systems and in quantum dots. It is possible to demonstrate that the structure of the matrix elements $g_{s,s'}$ and the $j_{s,s'}^{\pm}$, for semicylindrical QWR (see Appendix), produces twofold degeneracies of all states and, thus, the energy splitting $\Delta_{n,m}^{(1)}$ and $\Delta_{n,m}^{(3)}$ are identically zero. This is clearly represented in Fig. 6 where the total values of

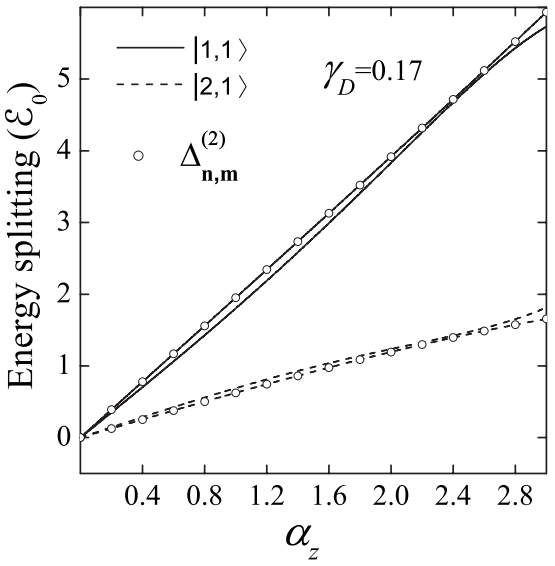

FIG. 6. Energy splitting $\Delta_{1,1}$ (solid line) and $\Delta_{2,1}$ (dashed line) for a semicylindrical QWR, in units of $\mathcal{E}_0$, as a function of the dimensionless wave vector α_z for fixed γ_D=0.17. The effect of SOI quadratic BIA terms is indicated by circles. The linear and cubic Dresselhaus SOI contributions to the energy splitting are zero.

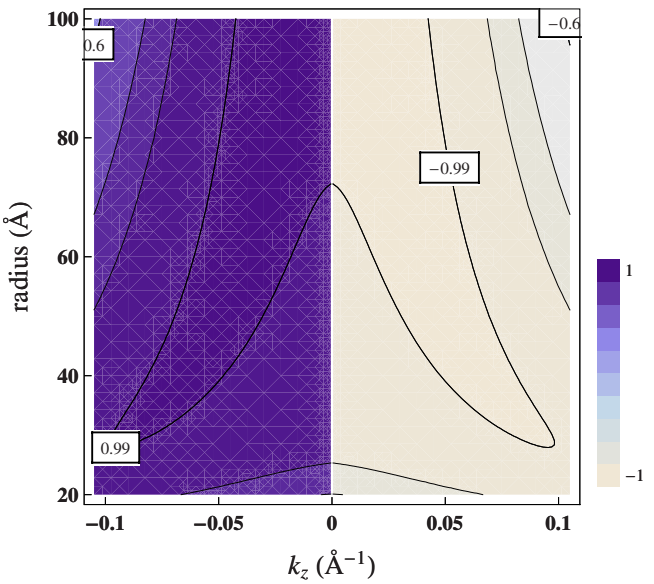

FIG. 7. (Color online) Spin-polarization contours (k_z versus radius a), $\bar{\sigma}_z(1,1)$, for the ground-state for a semicylindrical QWR with Dresselhaus strength $2m\beta/\hbar^2$=5 Å. For $k_z>0$ ($k_z<0$) the ground state corresponds to the state $|1,1;-\rangle$ ($|1,1;+\rangle$).

the spin splitting $\Delta_{1,1}$ and $\Delta_{2,1}$ are compared with the splitting produced by the quadratic intraspin terms, $\Delta^{(2)}_{1,1}$ and $\Delta^{(2)}_{2,1}$, for fixed Dresselhaus parameter, γ_D=1.7, as a function of α_z. The Zeeman-type quadratic contribution from $\mathcal{H}_{2D}$ is always additive, while the $\mathcal{H}_{1D}$ and $\mathcal{H}_{3D}$ terms, although inducing mixtures of spinor components, still exhibit a negligible contribution to the energy splitting for any value of the wave vector k_z or any Dresselhaus coupling parameter γ_D. The enhancement of the spin-splitting energy is almost linear with increasing $\alpha_z \propto k_z$, as can be expected from the definition of the $\mathcal{H}_{2D}$ interaction Hamiltonian in Eq. (2).

The spin polarization of energy levels, $\bar{\sigma}_z(1,1)$ $[\bar{\sigma}_z(n,m) = \langle\psi_{n,m}|\hat{S}_z|\psi_{n,m}\rangle / |\langle\psi_{n,m}|\psi_{n,m}\rangle|]$ is depicted in Fig. 7 as contour plots of k_z versus the radius of semicylindrical QWR, a. As mentioned, states subjected to SOI are invariant under simultaneous inversion operations, $k_z \Leftrightarrow -k_z$ and $\sigma_z \Leftrightarrow -\sigma_z$, being the mirrorlike images for the ground state shown in Fig. 7. Thus, according to Figs. 5 and 7, the ground state $|1,1;-\rangle$ has $k_z>0$, while for $k_z<0$ the state with lower energy is $|1,1;+\rangle$. These states represent electrons that travel freely along positive ($k_z>0$) and negative ($k_z<0$) z directions, with average spin polarizations parallel and antiparallel to the wire axis or, more specifically, $\bar{\sigma}_z(1,1)|_{(+k_z)} = -\bar{\sigma}_z(1,1)|_{(-k_z)}$. As it was stated above, the Zeeman-type $\mathcal{H}_{2D}$ intraspin term does not mix spin components of spinor states but produces the largest spin splitting, $\Delta^{(2)}_{n,m}$. The $\mathcal{H}_{1D}$ and $\mathcal{H}_{3D}$ interspin terms couple spin-up and spin-down components of spinor, thus affecting $\bar{\sigma}_z(n,m)$, although they produce exactly no contribution to spin splitting, $\Delta^{(1)}_{n,m} \equiv \Delta^{(3)}_{n,m} \equiv 0$. Therefore, we are able to obtain almost pure spin ground state for almost all relevant values of the radius a, which show spin polarization near or larger than 99% in a broad interval of $k_z \in (-0.02, 0.02)$ Å^{-1}, as shown in Fig. 7. For the range $|k_z|>0.05$ Å and increasing values of a, the ground states of semicylindrical QWRs exhibit a percentage increasing mixtures of spin-up and spin-down pure states and thus, the spin polarizations $\pm\bar{\sigma}_z(1,1)$ reach values below 90% (see Fig. 7).

IV. SUMMARY AND CONCLUSIONS

The Dresselhaus SOI in semiconductor QWRs shows strong dependence on the geometry of the confinement and the BIA-induced effects on the energy eigenvalues, spin-split energy levels, and spin polarizations that can be tracked for linear, quadratic, and cubic terms or $\mathcal{H}_{1D}$, $\mathcal{H}_{2D}$, and $\mathcal{H}_{3D}$ in Eq. (2), respectively. We have studied the importance of considering full BIA contributions in cylindrical and semicylindrical cross-section QWRs. In both cases, the most important contribution to spin-polarized states, $|1,1;\pm\rangle$, comes from the $\mathcal{H}_{2D}$ term which is responsible for the gap opened between the twofold spin-degenerate levels. The $\mathcal{H}_{3D}$ interaction has particularly significant effects on the excited states $|2,1;\pm\rangle$. In contrast, the linear-BIA term affects the spin polarization, $\bar{\sigma}_z(n,m)$, but has negligible effects to the energy levels and their spin splitting. Although the intraspin $\mathcal{H}_{2D}$ term vanishes in systems where $\langle\hat{k}_z\rangle \equiv 0$ (QW and QD), for QWRs the wave vector k_z is a good quantum number and its effect on spin polarization and spin splitting of states becomes more significant than the effects produced by $\mathcal{H}_{1D}$ and $\mathcal{H}_{3D}$ terms. Moreover, $\mathcal{H}_{3D}$ is independent of k_z and $\mathcal{H}_{1D}$ depend on k_z^2, thus, the effects produced by these interspin SOI terms may reach similar magnitudes; however the value of k_z where both terms have comparable values will depend on the state under consideration (see Fig. 3 for the QWR case).[17] These observations are also dependent on the geometry. Cylindrical QWR ground level is twofold degenerate with planar angular momentum quantum number n=0 and

$m=1$, whereas the semicylindrical QWR symmetry, fulfilling the boundary conditions in Eq. (5), forbids the presence of states with $n \leq 0$. Therefore, under this geometry neither $\mathcal{H}_{1\mathcal{D}}$ nor $\mathcal{H}_{3\mathcal{D}}$ contributes to the energy spin splitting besides leaving the states twofold degenerate. As seen in Fig. 5(b), their effects produce only small shifts to the energy levels.

Finally, the spin polarization of ground states of a semicylindrical QWR, $\bar{\sigma}_z(1,1)$, is qualitatively different from the cylindrical case due to different contributions induced by Dresselhaus SOI. For any level, there is not spin-degeneracy for a fixed value of k_z in contrast to the cylindrical case where there are always twofold spin-degenerate levels at any fixed value of k_z, regardless its propagation direction ($\pm z$). The semicylindrical confinement has given rise to an energy splitting of twofold degenerate levels of QWRs produced by the $H_{2\mathcal{D}}$ term, a dominant process that preserves spin polarization at small values of k_z. This opens the possibility of using low velocity ($v_z = \pm \hbar k_z / m^*$) transport measurements to explore preferential spin channels according to the sign (propagation direction) of induced spin-polarized currents in these quasi-1D nanostructures. Moreover, using this peculiar symmetry for the ground state in semicylindrical QWRs we can expect the formation of robust spin-filter devices. If electrons with energy $E/E_0 \lesssim 17$ are injected along the z axis of semicylindrical ensemble of parallel QWRs, this device can only transmit a high degree of spin-up current in direction $+z$ and opposite spins in the $-z$ direction. A dominant spin-up or spin-down character of the current depends on the sign of the $\bar{\sigma}_z$, and the current density is directly linked to the interplay between the radius a and the wave vector $\mathbf{k}_z$, as seen in Fig. 7. The ratio $2m\beta/\hbar^2 = 5$ Å, used in Fig. 7, corresponds to totally realistic values for InAs semiconductors.[18] For cylindrical radius $30 \leq a \leq 60$ Å and $0 < k_z < 0.5$ Å^{-1}, it is possible to get more than 90% degree of spin-polarized currents in the independent spin-up and spin-down channels. These results are based solely on the spatial symmetry properties of the quasi-one-dimensional nanostructures and enable realization of spin filters and tuned spin-polarized current densities in both parallel QWR directions. Also, combination of parallel wires may be used to generate logical gates, necessary for quantum information transmission and spintronic devices.

It is worth commenting on another SOI contribution provoked by the structural inversion asymmetry in nanostructure, the so-called Rashba interaction. The Rashba spin-splitting Hamiltonian, $\mathcal{H}_R = \alpha \mathbf{k} \times \nabla V \cdot \sigma$,[19] in a material with coupling parameter α is associated to spatial asymmetries of the lateral confinement potential, $V(x,y)$. This contribution is linear on $\mathbf{k}$ components and presents the same mathematical structure as the $\mathcal{H}_{1\mathcal{D}}$ term. It is clear that eigenstates of $\mathcal{H}_0 + \mathcal{H}_R$ are also eigenstates of $\mathcal{H}_0 + \mathcal{H}_{1D}$. The effect of this term adds to the linear Dresselhaus SOI, (for more detailed discussion see Ref. 11). For fixed SO-coupling constant, the spin splitting induced by $\mathcal{H}_{1D}$ is positive (see Figs. 3 and 6), whereas for $\mathcal{H}_R$ the splitting $\Delta^{(1)}_{n,m}$ has negative values. Therefore, the net effect of $\mathcal{H}_{1D} + \mathcal{H}_R$ is to minimize the contribution from $\mathcal{H}_{1D}$ and decrease the values of $\Delta^{(1)}_{n,m}$.[11] Moreover, the efficiency of the proposed spin-filter devices should decline for high impurity concentration or under strong current density injection where the electron-electron interaction becomes important. The validity of our proposition is directly linked to the conservation of the wave vector k_z. In this sense, these two effects break translational invariance along the z axis and the single-particle problem based on k_z conservation would require another formulation.

ACKNOWLEDGMENTS

This work was partially supported by CONACYT/Mexico and Brazilian agencies FAPESP, CNPq, and FAPEMIG. L.V-L wants to thank E. Gomez and H. Tsuzuki for technical assistance. G.E.M. and C.T-G. are grateful for the Visiting Scholar Program of the ICTP/Trieste.

APPENDIX: SPIN ORBIT TERMS

The matrix elements $g^{\pm}_{s,s'}$, $h_{s,s'}$, and $j^{\pm}_{s,s'}$ are necessary in order to build the Hamiltonian matrix (9) for the BIA SOI. In polar coordinates the operators $\hat{k}_{\pm}$ are written as

$$\hat{k}_{\pm} = -ie^{\pm i\varphi}\left(\frac{\partial}{\partial \rho} \pm \frac{i}{\rho}\frac{\partial}{\partial \varphi}\right). \tag{A1}$$

1. Cylindrical confinement

Using the wave functions [Eq. (6)] it is straightforward to show that

$$g^{\pm}_{s,s'} = a\langle s|\hat{k}_{\pm}|s'\rangle = \mp 2iT^{n,m}_{n',m'}\delta_{n',n\mp 1}, \tag{A2}$$

where $s=(n,m)$ and $s'=(n',m')$,

$$h_{s,s'} = a^2\langle s|\hat{k}^2_- + \hat{k}^2_+|s'\rangle = 4[(n+1)\delta_{n',n+2} - (n-1)\delta_{n',n-2}]T^{n,m}_{n',m'}, \tag{A3}$$

with

$$\lim_{n \mapsto \mp 1}\{\pm(n+1)T^{n,m}_{n\pm 2,m'}\} = 2\mu^2_{n,m}\delta_{m',m}, \tag{A4}$$

and for the cubic contribution we have

$$j^{\pm}_{s,s'} = a^3\langle s|\{\hat{k}^2_{\pm},(\hat{k}^2_+ - \hat{k}^2_-)\}|s'\rangle = \mp iT^{n,m}_{n',m'}\{2\mu^2_{n'm'}\delta_{n',n\pm 1} + [4(n' \pm 1)(n' \pm 2) - \mu^2_{n'm'}]\delta_{n',n\mp 3}\}, \tag{A5}$$

where

$$T^{n,m}_{n',m'} = \frac{\mu_{n,m}/\mu_{n',m'}}{(\mu_{n,m}/\mu_{n',m'})^2 - 1}. \tag{A6}$$

2. Semicylindrical confinement

Following Eq. (6) for the semicylindrical case we have that

$$g^{+}_{s,s'} = i\ \mathrm{sgn}(n-n')T^{n,m}_{n\pm 1,m'}, \quad \text{if } n' = n \pm 1, \tag{A7}$$

$$g^{+}_{s,s'} = \frac{2n}{\mu_{s'}\pi}\frac{1+(-1)^{n+n'}}{J_{n'+1}(\mu_{s'})J_{n'+1}(\mu_s)}F^{n,m}_{n',m'}, \quad \text{if } n' \neq n \pm 1, \tag{A8}$$

where $\mathrm{sgn}(x)=+1$ if $x>0$ and $\mathrm{sgn}(x)=-1$ if $x<0$ and $F^{s}_{s'}$ are numbers ruled by

$$F^{s}_{s'} = \int_0^{\mu_{s'}} zJ_n\left(\frac{\mu_s}{\mu_{s'}}z\right)\left[\frac{J_{n'-1}(z)}{(1-n')^2-n^2} - \frac{J_{n'+1}(z)}{(1+n')^2-n^2}\right]dz. \tag{A9}$$

In the particular case where $s=s'$ Eq. (A9) can be reduced to

$$F^{s}_{s} = \frac{2n}{(2n)^2-1}\int_0^{\mu_s}\left\{z\frac{d}{dz}[J_n(z)]^2 + [J_n(z)]^2\right\}dz$$

$$= \frac{2n}{(2n)^2-1}\int_0^{\mu_s}\frac{d}{dz}\{z[J_n(z)]^2\}dz = 0. \tag{A10}$$

Also, it follows the relation

$$g^{-}_{s,s'} = (-1)^{n'+n+1}g^{+}_{s,s'}. \tag{A11}$$

The other matrix elements for the semicylindrical QWR, $h_{s,s'}$ and $j^{\pm}_{s,s'}$, are evaluated numerically using Eqs. (A7)–(A11) and the matrix identity $\langle s|\hat{A}\hat{B}|s'\rangle = \Sigma_p\langle s|\hat{A}|p\rangle\langle p|\hat{B}|s'\rangle$.

[1] R. H. Parmenter, Phys. Rev. **100**, 573 (1955).

[2] G. Dresselhaus, Phys. Rev. **100**, 580 (1955).

[3] A detailed analysis, including all three Dresselhaus contributions for the twofold lowest subbands in zinc-blende bulk structures, has been carried out in G. E. Marques, A. C. R. Bittencourt, C. F. Destefani, and S. E. Ulloa, Phys. Rev. B **72**, 045313 (2005).

[4] R. Winkler, *Spin-Orbit Coupling Effects in Two-Dimensional Electron and Hole Systems, Springer Tracts in Modern Physics* (Springer, Berlin, 2003), Vol. 191, and references therein.

[5] H. B. de Carvalho, M. J. S. P. Brasil, V. Lopez-Richard, Y. Galvao Gobato, G. E. Marques, I. Camps, L. C. O. Dacal, M. Henini, L. Eaves, and G. Hill, Phys. Rev. B **74**, 041305(R) (2006); see also L. F. dos Santos, Y. G. Gobato, V. Lopez-Richard, G. E. Marques, M. J. S. P. Brasil, M. Henini, and R. J. Airey, Appl. Phys. Lett. **92**, 143505 (2008).

[6] S. Gopalan, J. K. Furdyna, and S. Rodriguez, Phys. Rev. B **32**, 903 (1985).

[7] F. G. Pikus and G. E. Pikus, Phys. Rev. B **51**, 16928 (1995).

[8] J. Schliemann, J. C. Egues, and D. Loss, Phys. Rev. Lett. **90**, 146801 (2003); S. Bandyopadhyay, S. Pramanika, and M. Cahay, Superlattices Microstruct. **35**, 67 (2004); S. Kettemann, Phys. Rev. Lett. **98**, 176808 (2007).

[9] G. Fasol and H. Sakaki, Phys. Rev. Lett. **70**, 3643 (1993).

[10] F. M. Alves, G. E. Marques, V. Lopez-Richard, and C. Trallero-Giner, Semicond. Sci. Technol. **22**, 301 (2007).

[11] F. M. Alves, C. Trallero-Giner, V. Lopez-Richard, and G. E. Marques, Phys. Rev. B **77**, 035434 (2008).

[12] C. F. Destefani, S. E. Ulloa, and G. E. Marques, Phys. Rev. B **69**, 125302 (2004).

[13] F. Malet, M. Pi, M. Barranco, L. Serra, and E. Lipparini, Phys. Rev. B **76**, 115306 (2007).

[14] S. Pramanik, S. Bandyopadhyay, and M. Cahay, Phys. Rev. B **68**, 075313 (2003).

[15] D. M. Zumbühl, J. B. Miller, C. M. Marcus, D. Goldhaber-Gordon, J. S. Harris, Jr., K. Campman, and A. C. Gossard, Phys. Rev. B **72**, 081305(R) (2005).

[16] J. J. Krich and B. I. Halperin, Phys. Rev. Lett. **98**, 226802 (2007).

[17] These results are independent of the lateral confining potential used to describe the in-plane localization in cylindrical QWRs. If another two-dimensional confining potential is employed instead of the hard-wall model, the stronger spin-splitting effect still comes from the quadratic Dresselhaus term since the translational symmetry is preserved along wire axis.

[18] Parameters for InAs semiconductor $m^*/m_0=0.0229$ from Landolt-Börnstein Comprehensive Index, edited by O. Madelung and W. Martienssen (Springer, Berlin, 1996) and $\beta=27.18$ eV Å^3 from Ref. 4.

[19] Yu. A. Bychkov and E. I. Rashba, Sov. Phys. JETP **39**, 78 (1984); J. Phys. C **17**, 6039 (1984).